IJCSE International Journal of Computer Sciences and Engineering Open Access
Research Paper Vol.-6, Issue-7, July 2018 E-ISSN: 2347-2693

Doa Estimation of Broad-Banded Linear and Quadratic Chirps Using Nested and Co-Prime Arrays

G. Sreekumar[1*], Leena Mary[2], A. Unnikrishnan[1]

[1*]Dept. of E.C.E., Rajagiri School of Engg. and Tech. & M. G. University, Kerala, India.
[2] Dept. of E.C.E., Govt. Engg. College, Idukki ,Kerala, India.
[1] Principal, Rajagiri School of Engg. and Tech., Kerala, India.

[*]*Corresponding Author: ggsreekumar80@gmail.com, Tel.: +91-9895505668*

Available online at: www.ijcseonline.org

Accepted: 20/Jul/2018, Published: 31/July/2018

***Abstract*—** Detection and localization of active and passive targets using sensor arrays play an important role in the field of array signal processing. In this paper the problem of estimating the direction of arrivals of broad banded linear and quadratic chirp sources using both nested and co-prime arrays is addressed. Traditional uniform arrays can only detect N-1 number of sources with N physical sensors using high resolution beam formers like MUSIC. However the nested and co-prime arrays can detect more number of sources than the number of sensors by exploiting the difference co-array structure based on the correlation of the observations. Difference co-array is the distinct sensor locations obtained by taking all possible pairwise differences of sensor locations in the original array. As the chirp signal, commonly used in both radar and sonar systems is better processed in the fractional Fourier domain, the detection is done using fractional Fourier transform (FrFT). But as the traditional FrFT is limited to the analysis of linear chirps, detection using modified FrFT is found to be the apt choice for quadratic chirps. Subsequently, the direction of arrival estimation is achieved using subspace methods which include MUSIC and minimum-norm in the proposed work. The effectiveness of the algorithm is validated through different signals including real data obtained from a practical sonar array. It is seen from the computer simulations that nested-MUSIC combination has better resolution and accuracy than all other combinations.

***Keywords*—**Direction of arrival estimation, Fractional Fourier transform, Chirp sources, Nested array, Coprime array.

I. INTRODUCTION

Array signal processing has been an active area of research employed in a wide variety of applications such as radars [1], sonars [2], communication [3] etc. This includes detection and parameter estimation of active and passive targets using an array of sensors separated in space. Such problems promise high SNR gain through beam-forming, in the context of direction of arrival (DoA) estimation. The DoA estimation method which is found to be very effective for narrow-band signals is the conventional beam-former (CBF) that does delay-sum operation [4]. But it is found that CBF involves high side lobe levels and hence it is not very effective in resolving multiple sources. Capon et al. [5] developed the minimum variance distortionless look (MVDL) by modifying the CBF weights to improve the resolution. As this algorithm involves the requirement of inverting the full-rank spatial covariance matrix dimensioned by the size of the aperture, it is found to be computationally complex. Subspace based methods also result in the high resolution of multiple targets which include multiple signal classification (MUSIC) [6], root-MUSIC [7], minimum norm (MN) [8] and the estimation of signal parameters via rotational invariance techniques (ESPRIT) [9].

Chirps are signals which exhibit a change in instantaneous frequency with time and are of particular interest in active and passive systems of radars [10] and sonars [11]. The applications also span other areas which include ultrasonic imaging, acoustic communications and seismic surveying. Natural chirp signals exist in the form of whistles produced by dolphins, whales, birds and bats. These sounds are modelled as either linear frequency modulated (LFM) chirps or non-linear versions which include quadratic frequency modulated (QFM) and hyperbolic frequency modulated (HFM) waveforms. For passive sensor arrays, the chirp signals are produced due to Doppler effect when the sinusoidal source is accelerating [12]. Some active radars and sonars system use chirp signals for transmission, providing good detection response of low Doppler targets with long range resolution [13].

Traditional methods of DoA estimation cannot be used as such for chirp sources because the array response vector is

continuously changing with time. Passive chirps follow the usual approach of separating the data into several narrow-band frequency bins and perform the DoA estimation for each frequency bin, where the final estimate is the statistical average of all bins [14], [15]. In the case of active chirp, each frequency is focused to a reference focusing frequency and then a single correlation matrix is obtained by adding these focused correlation matrices, to which the traditional DoA estimation methods could be applied [16], [17], [18]. But the performance of first method suffers severely at low SNR, while the other method is likely to depend on the selection of the focusing frequency [19]. In this context, for the chirping signals, the beam-forming using fractional Fourier transform (FrFT), where the FrFT parameters are chosen based on the chirp signal, can improve the performance of DoA estimation in terms of computational efficiency, accuracy and resolution. Also by using FrFT, the detection at low SNR gets improved, since the FrFT with the matching parameters, converts the broad-band signal into its narrow-band representation in the fractional domain.

FrFT is a linear transformation having low computational complexity and high noise resilient property [20]. It extends the capabilities of conventional Fourier transform and decomposes the signal into an orthonormal basis of linear chirps. As the process involved is the linear rotation of the time-frequency plane, the use of FrFT is limited to the class of linear chirps. Therefore new techniques need to be developed for non-linear chirps. Sahay *et al.* [21] introduced the modified FrFT called the 'generalized time frequency transform' (GTFT) for the analysis of higher order chirps. The kernels of FrFT and other transforms such as Fresnel and affine transform can be obtained as a special case of GTFT [22]. But the parameters of the signal have to be searched for the incoming unknown chirps which becomes a tedious task. The parameter search problem becomes too complex for the higher order chirps as the number of parameters of a given chirp is proportional to the order number. The polynomial curve fitting can solve the problem to some extend since the parameters of the chirp are related to the coefficients of the polynomial representing the chirp. Peng *et al.* developed a new time-frequency representation in this regard known as polynomial chirplet transform (PCT) [23] which can extract the coefficients of both linear and nonlinear chirps. PCT is a modified version of the conventional chirplet transform (CT) [24] as the latter fails to analyze the nonlinear chirps.

Traditional uniform arrays such as uniform linear array (ULA), uniform planar array (UPA) and uniform circular array (UCA) can only detect N-1 number of sources using N number of physical sensors. Therefore additional sensors are required to detect more number of sources which will increase computational complexity and cost. The sparse linear arrays such as nested [25] and co-prime [26] arrays have the attractive capability of providing enhanced degrees of freedom. Therefore these are capable of resolving more sources than the number of sensors by exploiting the so called "difference co-array" based on the correlation of the observations. Difference co-array is the distinct sensor locations obtained by taking all possible pairwise differences of sensor locations in the original array. By exploiting the co-array structure, an augmented sample covariance matrix can be constructed and subspace methods can be applied to identify more sources than the number of sensors. The traditionally used ULA which is analogous to uniform sampling is found unsuitable as the difference co-array is not creating any additional element with respect to the original array.

In this paper, the DoA estimation of broad banded linear and quadratic frequency modulated chirps using nested and co-prime arrays is presented. The analysis is done using simulated chirps as well as real data obtained from a practical sonar array. As conventional FrFT is limited to the analysis of linear chirps, detection using modified FrFT is found to be the apt choice for higher order chirps by the proper selection of the kernel. The parameters of the quadratic chirp signal is extracted using the PCT approach and the DoA estimation is compared using various subspace methods.

The rest of the paper is organized as follows. In Section II, the signal model for LFM chirp sources is presented, in terms of the FrFT. Then the modified signal model based on difference co-array is mentioned in Section III. Subspace DoA estimation methods based on FrFT is discussed in Section IV. Extension of these ideas to QFM chirps is mentioned in section V. In Section VI, the numerical results of the performance of the DoA estimation methods are presented for different signals including real data obtained from a practical sonar array. The conclusions and directions for further work are summarized in Section VII.

Notations: Matrices are denoted by uppercase letters in boldface (e.g., **A**). Vectors are denoted by lowercase letters in boldface (e.g., **a**). Superscript ^{H} denotes Hermitian or transpose conjugate. The symbol $j = \sqrt{-1}$ denotes the imaginary part of a complex number.

II. SIGNAL MODEL FOR LFM SOURCES

Nested array is a chain of two ULAs specified by the following sensor array arrangement

$$Sn = \{1, 2, \ldots, N_1, (N_1+1), 2(N_1+1), \ldots N_2(N_1+1)\} \quad (1)$$

Out of the total sensors, half of the sensors upto N_1 form a ULA with unit distance spacing and the next half of the sensors are spaced directly proportional to the number of sensors in the first half [25]. By placing the antenna elements in this fashion, effect of first ULA can be recreated in between second ULA.

Co-prime array is a combination of two ULAs which utilizes the properties of co-prime pair of numbers given by

$$Sc = \{0, C, 2C, \ldots, (D-1)C, D, 2D, \ldots, (2C-1)D\} \quad (2)$$

Here C and D are chosen as the co-prime pair. The first uniform sub array will have D number of sensors with C unit distance and the second uniform linear sub array will have 2C number of sensors spaced at D unit distance making a total of 2C+D-1 senors for the co-prime array [26].

Assume P broad-band LFM chirp signals from directions θ_1, θ_2, ... θ_P impinging on a sparse array given by (1) or (2) having a total of N isotropic non-uniform linear antenna array elements. The time series of data at the q^{th} sensor is given by

$$x_q(t) = \sum_{i=1}^{P} s_i\left(t - \tau_q(\theta_i)\right) + n_q(t) \quad (3)$$

where $\tau_q(\theta_i)$ is the time delay of the i^{th} broadband chirp at the q^{th} sensor given by

$$\tau_q(\theta_i) = \left(\frac{d_q}{v}\right)\sin\theta_i \quad (4)$$

The sensors are placed on a linear grid with d_q denoting the position of the q^{th} sensor which is an integer multiple of the smallest spacing, d_{min} in the underlying grid. The parameter 'v' represents the signal speed and the spacing d_{min} is taken as $\lambda_{min}/2$ to prevent aliasing in the spacing domain where λ_{min} is the minimum wavelength of the combined incoming sources.

The broad-banded linear chirp is represented by the following equation

$$s(t) = \exp\left[j2\pi\left(bt^2 + f_0 t + c\right)\right] \quad (5)$$

where *'b'* is the chirp rate, f_0 is the start frequency and *'c'* is the initial phase of the chirp. The term $bt^2 + f_0t + c$ defines the phase and its first derivative $2bt + f_0$ represents the instantaneous frequency (IF). Therefore three parameters define a linear chirp completely viz. start frequency, chirp rate and the duration over which *'t'* is defined.

In frequency domain representation the received data vector in (3) with the broad-banded signal as input has the form

$$\mathbf{x}(f_k) = \mathbf{A}(\theta, f_k)\mathbf{s}(f_k) + \mathbf{n}(f_k) \quad (6)$$

where $\mathbf{A}(\theta, f_k) = [\mathbf{a}(\theta_1, f_k)\ \mathbf{a}(\theta_2, f_k) \ldots\ \mathbf{a}(\theta_D, f_k)]$ represents the array steering matrix for the k^{th} bin and $\mathbf{a}(\theta_i, f_k)$ is the steering vector of the i^{th} source represented as

$$\mathbf{a}(\theta_i, f_k) = \left(1 \quad \exp\left(-j2\pi f_k d_2 \frac{\sin\theta_i}{v}\right) \quad --- \quad \exp\left(-j2\pi f_k d_N \frac{\sin\theta_i}{v}\right)\right)^T \quad (7)$$

$\mathbf{s}(f_k) = [s_1(f_k)\ s_2(f_k) \ldots\ s_D(f_k)]^T$ represents the k^{th} FFT coefficient of the signal vectors and that of noise is given by $\mathbf{n}(f_k) = [n_1(f_k)\ \ n_2(f_k) \ldots\ n_N(f_k)]^T$. The term $\mathbf{A}(\theta, f_k)\mathbf{s}(f_k)$ represents inverse beam-forming vector which delays the plane wave to reach the spatially separated sensors.

The FrFT is a time varying filter and is a one parameter generalization of the classical Fourier transform. Namias introduced the idea of FrFT in the area of quantum mechanics for the solution of differential equation problems [27]. The discrete implementation of FrFT was put forward by Ozaktas [28] where the fractional transform is broken into a chirp multiplication followed by a chirp convolution followed by another chirp multiplication. Since then, a number of applications have been developed, mostly in the field of optics [29]. Recently it has been applied to the area of sensor arrays [30], [31].

The FrFT of a signal *s(t)* is defined as

$$S_\phi(u) = F_\phi[s(t)] = \int_{-\infty}^{+\infty} K_\phi(t,u)s(t)dt \quad (8)$$

where ϕ is the anticlockwise rotation angle of the transform varying from 0 to $\pi/2$. When $\phi = \pi/2$, FrFT reduces to the classical Fourier transform and the inverse FrFT is obtained by substituting $\phi = -\pi/2$. *'p'* is the order of FrFT, which can be any real number between 0 and 1 and is related to the rotation angle as $\phi = p\pi/2$.

$K_\phi(t,u)$ is the kernel of the FrFT defined as:

$$K_\phi(t,u) = S_\phi \exp\left[j\pi\left(\left(t^2 + u^2\right)\cot\phi - 2tu\csc\phi\right)\right] \quad (9)$$

where $S_\phi = \sqrt{1 - j\cot\phi}$.

The relationship between the chirp rate 'b' and the optimum order p_{opt} is given by

$$p_{opt} = \frac{2\phi}{\pi} = \frac{2}{\pi}\tan^{-1}\left(\frac{1}{2b}\right) \quad (10)$$

However the true relationship depends on the digital sampling scheme [32], [33] used and is given by

$$p_{opt} = \frac{2}{\pi}\tan^{-1}\left(\frac{f_s^2}{2bM}\right) \quad (11)$$

where *fs* is the sampling frequency and M is the number of samples. Conversely, given the true order, this can be used to compute the chirp rate. A one-dimensional search is required to find the optimum order for unknown signals in the case of passive sensor arrays, whereas for active arrays the complete information is available with the transmitter [20].

Using (8), the FrFT of the chirp signal represented in (5) with zero initial slope can be obtained as

$$S_\phi(u) = F_\phi[s(t)] = S_\phi \exp\left[j\pi\left(u^2\cot\phi\right)\right] \times \int_0^T \exp\left[j\pi t^2\left(\cot\phi + 2b\right)\right]\exp\left[j2\pi t\left(f_0 - u\csc\phi\right)\right]dt \quad (12)$$

where T is the pulse width of the chirp. The chirp signal represented at its optimum order produces impulses which is given by the peak point of (12). The theoretical peak point which transforms the natural frequency to fractional frequency is given by $u = (f_0 + bT)\sin\phi = f_{mid}\sin\phi$ where f_{mid} represents the mid-frequency of the incoming chirp.

Also (12) represents the FrFT of the chirp signal at the first sensor which is the reference sensor. For the q^{th} sensor, the FrFT of the i^{th} signal which is delayed by $\tau_q(\theta_i)$ can be obtained as per the property of FrFT as

$$F_\phi\left[s_i\left(t-\tau_q(\theta_i)\right)\right]=S_\phi\left(u-\tau_q(\theta_i)\cos\phi\right)\times \exp\left[j\pi\left(\tau_q^2(\theta_i)\sin\phi\cos\phi-2u\tau_q(\theta_i)\sin\phi\right)\right] \quad (13)$$

As the time delay between two sensors $\tau_q(\theta_i)$ is a small value and so also is its square, the above equation can be approximated as

$$F_\phi\left[s_i\left(t-\tau_q(\theta_i)\right)\right]=S_\phi(u)\times\exp\left[-j2\pi(q-1)u\tau(\theta_i)\sin\phi\right] \quad (14)$$

Therefore the array steering vector for the N sensors in the FrFT domain can be written in terms of $\delta = 2\pi u\tau(\theta_i)\sin\phi$ as

$$\mathbf{a}_\phi(\theta_i,u)=\left(1 \quad \exp[-j\delta] \quad --- \quad \exp\left[-j2\pi f_k d_N\frac{\sin\theta_i}{v}\right]\right)^T \quad (15)$$

III. MODIFIED SIGNAL MODEL BASED ON DIFFERENCE CO-ARRAY

As the sensor array of interest is non-uniform in nature, subspace methods like MUSIC cannot be directly applied to find the direction information. But it was found that uniformity is observed in the difference co-array domain because of the special array structure employed in both nested and co-prime arrays [25], [26]. In the difference co-array structure, it is found that all the missing sensor locations are recreated and hence the aperture is expanded. This results in more degrees of freedom so that more number of sources can be detected with less number of sensors, unlike ULA which is not capable of creating new additional points in the co-array. As the covariance sequence depends only on the difference in the sampling instances, converting the data to their second order statistics can build the difference co-array.

The spatial covariance matrix of the sensor output in the FrFT domain is given by

$$\mathbf{R}_\mathbf{x}(u)=E\left(\mathbf{x}(u)\mathbf{x}^H(u)\right)=\frac{1}{L}\sum_{l=1}^{L}\mathbf{x}_l(u)\mathbf{x}_l^H(u) \quad (16)$$

The dimension of $\mathbf{R}_\mathbf{x}$(u) is NxN as $\mathbf{x}$(u) is an Nx1 vector because of N physical sensors. Here L is the number of data blocks taken having T duration each which is the chirp pulse width and $\mathbf{x}_l(u)$ is the FrFT of the l^{th} chirp block. However as the FrFT of the chirp signal at its optimum order produces impulse at u_{opt} irrespective of the bandwidth, it is worth enough to take the peak point alone to calculate $\mathbf{R}_\mathbf{x}$(u) as the other values are all negligible or zeros in the fractional domain. The matrix $\boldsymbol{R}_\mathbf{x}(u)$ is vectorized to yield a long vector $\tilde{\mathbf{x}}(u)$ which is precisely the difference co-array of the original array. The method of vectorization is numerically explained by taking a nested array with N = 4 (N_1, N_2 = 2). The resulting covariance matrix $\boldsymbol{R}_\mathbf{x}(u)$ showing the entries as $r(i,j)$ with the difference in the spatial sampling instances $(i-j)$ as subscript is shown in (17).

$$\mathbf{R}_\mathbf{x}(u)=\begin{bmatrix} r(1,1)_0 & r(1,2)_{-1} & r(1,3)_{-2} & r(1,6)_{-5} \\ r(2,1)_1 & r(2,2)_0 & r(2,3)_{-1} & r(2,6)_{-4} \\ r(3,1)_2 & r(3,2)_1 & r(3,3)_0 & r(3,6)_{-3} \\ r(6,1)_5 & r(6,2)_4 & r(6,3)_3 & r(6,6)_0 \end{bmatrix} \quad (17)$$

Here all the differences in the spatial sampling instances from -5 to 5 are created, giving the effect of a virtual ULA (difference co-array) $\tilde{\mathbf{x}}(u)$ of size 11x1 given by

$$\tilde{\mathbf{x}}(u)=\left[r(.)_{-5} \quad r(.)_{-4} \quad -- \quad r(.)_0 \quad -- \quad r(.)_4 \quad r(.)_5\right]^T \quad (18)$$

The entries corresponding to the same sensor separation is averaged to avoid redundancy. For example, the central element $r(.)_0$ is given by the average of five entries in the covariance matrix given by

$$r(.)_0=\left(\frac{r(1,1)_0+r(2,2)_0+r(3,3)_0+r(4,4)_0+r(5,5)_0}{5}\right) \quad (19)$$

To estimate the DoAs a Hermitian Toeplitz matrix $\tilde{\mathbf{R}}(u)$ given by (20) is constructed from $\tilde{\mathbf{x}}(u)$ [34]. $\tilde{\mathbf{R}}(u)$ is a positive semi-definite matrix suitable for the subspace decomposition.

$$\tilde{\mathbf{R}}(u)=\begin{bmatrix} r(.)_0 & r(.)_{-1} & r(.)_{-2} & r(.)_{-3} & r(.)_{-4} & r(.)_{-5} \\ r(.)_1 & r(.)_0 & r(.)_{-1} & r(.)_{-2} & r(.)_{-3} & r(.)_{-4} \\ r(.)_2 & r(.)_1 & r(.)_0 & r(.)_{-1} & r(.)_{-2} & r(.)_{-3} \\ r(.)_3 & r(.)_2 & r(.)_1 & r(.)_0 & r(.)_{-1} & r(.)_{-2} \\ r(.)_4 & r(.)_3 & r(.)_2 & r(.)_1 & r(.)_0 & r(.)_{-1} \\ r(.)_5 & r(.)_4 & r(.)_3 & r(.)_2 & r(.)_1 & r(.)_0 \end{bmatrix} \quad (20)$$

IV. METHODS OF DIRECTION OF ARRIVAL ESTIMATION

The DoA estimation using subspace methods include MUSIC [6] and MN [8] methods. The spatial energy spectrum for MUSIC and MN beam-formers can be re-casted in the following way for chirp signals represented in FrFT domain.

$$E_{MUSIC}(\theta)=\frac{1}{\mathbf{a}_p^H(\theta,u)\mathbf{U}_n\mathbf{U}_n^H\mathbf{a}_p(\theta,u)} \quad (21)$$

$$E_{MN}(\theta)=\frac{1}{\mathbf{a}_p^H(\theta,u)\mathbf{U}_n\mathbf{U}_n^H\mathbf{e}} \quad (22)$$

where **e** is a vector of all zeros except a 1 at the first position and $\mathbf{U}_n$ is the noise eigenvector obtained from the eigen decomposition of $\tilde{\mathbf{R}}(u)$, the Hermitian Toeplitz matrix given by (20).

V. EXTENSION TO QFM SOURCES

The quadratic frequency modulated (QFM) chirp is represented by the following equation

$$s(t) = \exp\left[j2\pi\left(at^3 + bt^2 + f_0 t + c\right)\right] \quad (23)$$

where *'a'* is the additional parameter w.r.t. LFM which controls the curvature of the quadratic chirp term. Here the IF trajectory of the signal is a non-linear function of time given by

$$f(t) = 3at^2 + 2bt + f_0 \quad (24)$$

The modified FRFT of the QFM signal *s(t)* is defined as

$$S_{\phi,\psi}(u) = F_{\phi,\psi}\left[s(t)\right] = \int_{-\infty}^{+\infty} K_{\phi,\psi}(t,u)s(t)dt \quad (25)$$

where $K_{\phi,\psi}(t,u)$ is the modified kernel for quadratic chirp given by

$$K_{\phi,\psi}(t,u) = S_\phi \exp\left[j\pi\begin{pmatrix}\left(t^2+u^2\right)\cot\phi - 2tu\csc\phi \\ -2tu\csc\phi - 2\psi t^3 + 2\psi u^3\end{pmatrix}\right] \quad (26)$$

The parameters are related to the polynomial coefficients as

$$a = \psi; b = \frac{f_s^2}{2M\tan\phi}; f_0 = u\csc\phi - bT \quad (27)$$

Therefore modified FrFT of the QFM chirp signal represented in (23) with zero initial slope is obtained as

$$F_{\phi,\psi}\left[s(t)\right] = S_\phi \exp\left[j2\pi\psi u^3\right] \times \int_{-\infty}^{+\infty} s(t) \times \exp\left[-j2\pi\psi t^3\right] \quad (28)$$
$$\exp\left[j\pi\left(\left(t^2+u^2\right)\cot\phi - 2tu\csc\phi\right)\right]dt$$

Therefore the following operations are implemented on the signal.

(i) Multiplication of the quadratic chirp *s(t)* with another quadratic chirp $\exp[-j2\pi\psi t^3]$ which results in a linear chirp to which conventional FrFT can be applied. The evaluation of the FrFT would result in a function of *'u'*.

(ii) Multiplication of the above function in *'u'* with another quadratic chirp $\exp[j2\pi\psi u^3]$.

Here the ψ and ϕ values which are proportional to the polynomial coefficients are searched over the range values which becomes a time consuming process. The coefficient values can also be extracted using the polynomial chirplet transform (PCT) approach [23], thus avoiding the search procedure.

Introducing a delay for the IF expression of QFM given by (24) yields

$$f(t-\tau) = 3at^2 + 2b't + f_0' \quad (29)$$

where the new chirp rate and start frequency get modified as $2b' = 2b - 6a\tau$ and $f_0' = f_0 + 3a\tau^2 - 2b\tau$ respectively; but the quadratic chirp parameter *'a'* remains unchanged. As $2b = \cot\phi$ given by (10) and because of the shift in the start frequency, the rotation angle and peak value changes to β and *u'* respectively as shown below.

$$\cot\beta = \cot\phi - 6a\tau \quad (30)$$

$$u'\csc\beta = u\csc\phi + 3a\tau^2 - \tau\cot\phi \quad (31)$$

Result: The array steering vector for the i^{th} source in the modified FrFT domain can be written as

$$\mathbf{a}_{\beta,\psi}(\theta_i, u') = \exp\left[j\pi\begin{pmatrix}u^2\cot\phi + 2\psi u^3 - 2u\boldsymbol{\tau}(\theta_i)\csc\phi \\ +\boldsymbol{\tau}^2(\theta_i)\cot\phi - 2\psi\boldsymbol{\tau}^3(\theta_i) \\ -u'^2\cot\beta - 2\psi u'^3\end{pmatrix}\right] \quad (32)$$

where $\boldsymbol{\tau}(\theta_i)$ is the inter-element delay vector for the N sensors whose q^{th} term is given by (4).

Proof : The proof is quite involved and can be found in [35].

VI. RESULTS AND DISCUSSION

A. *Simulated Sources*

Simulation experiments using seven LFM chirp sources *(C-1 to C-7)* of same bandwidth and different center frequencies with both nested and co-prime array configurations are discussed here. The sensor arrangement used for nested and co-prime arrays are denoted by Sn and Sc respectively as

$$\text{Sn} = \{1, 2, 3, 4, 8, 12\}\ ;\ \text{Sc} = \{0, 2, 4, 3, 6, 9\} \quad (33)$$

Table I shows the details regarding the chirp sources used where f_0 and f_1 represent the start and end frequencies respectively of the individual chirp. The sources are located at far field impinging on the sparse array with N = 6 sensors for both nested ($N_1 = N_2 = 3$) and co-prime (C = 2, D = 3) from DoAs *(-30^0, -20^0, -10^0, 0^0, 10^0, 20^0, 30^0)* with all equal power. The sampling frequency taken is 12,800 Hz with a total of 25610 time samples and the pulse width of chirp as 200 ms. The samples of the impinging signal are divided into L=10 blocks with each block having M = 2561 snapshots. In each block the 2561 samples are converted into FrFT which are then processed using the modified subspace beam-forming algorithms (21, 22). The signal is corrupted with an AWGN noise with SNR = -15 dB. The p_{opt} value is obtained as 0.9850 from (11) with chirp rate 750 Hz/s. The FrFT scheme involving MUSIC and MN beam-formers is able to clearly resolve seven sources which are closely located at very low SNR with only six physical sensors. This is clearly illustrated by Figure 1 and Figure 2 for nested and co-prime

arrays respectively. It can also be shown that using six sensors, nested array can resolve upto a maximum of 36 ($N^2 = 6^2$) sources, whereas co-prime array can only resolve 12 (2CxD = 4x3) sources. This is due to the peculiar array geometry of nested array creating a larger difference co-array in comparison with the co-prime array [34]. The high spatial energy is seen for MUSIC with both nested and co-prime cases and is reduced when it comes to MN.

Table 1. Chirp signals used for sparse array.

Chirp Signals	***C-1***	***C-2***	***C-3***	***C-4***	***C-5***	***C-6***	***C-7***
f_0 (Hz)	1000	1500	2000	2500	3000	3500	4000
f_1 (Hz)	1300	1800	2300	2800	3300	3800	4300

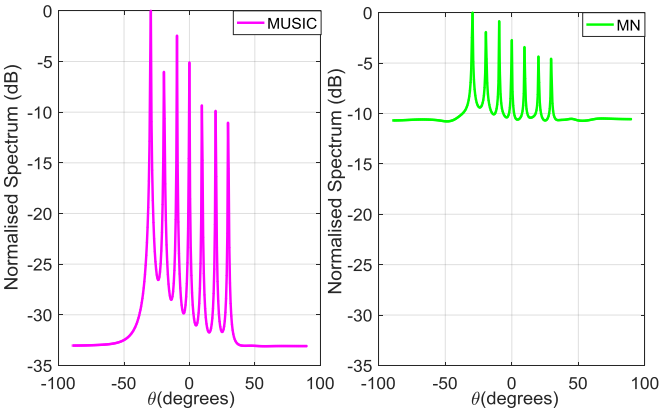

Figure 1. MUSIC and minimum norm energy spectrum using nested array for DoA estimation of seven chirp sources located at angles (-30^0, -20^0, -10^0, 0^0, 10^0, 20^0, 30^0) with FrFT beam-formers for N=6, L=10, SNR = -15dB.

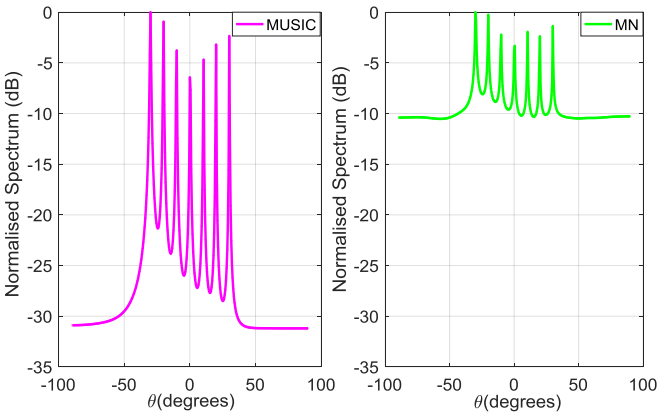

Figure 2. MUSIC and minimum norm energy spectrum using co-prime array for DoA estimation of seven chirp sources located at angles (-30^0, -20^0, -10^0, 0^0, 10^0, 20^0, 30^0) with FrFT beam-formers for N=6, L=10, SNR = -15 dB.

The beam-former performance is evaluated mainly using two factors - resolution and accuracy. The resolution is clearly evident from the energy spectrum plot and the accuracy is measured using root mean square error (RMSE) plot. The RMSE for the different DoA estimations is given by (34) where G and P represents the number of Monte-Carlo simulations and the number of sources respectively.

$$RMSE = \sqrt{\left(\frac{1}{G}\frac{1}{P}\sum_{g=1}^{G}\sum_{p=1}^{P}\left(\hat{\theta}_p(g) - \theta_p \right)^2 \right)} \quad (34)$$

$\hat{\theta}_p(g)$ is the estimation of the true angle θ_p for the g^{th} Monte Carlo trial. The variation of RMSE as a function of SNR for combined seven sources having azimuth angles $(-30^0, -20^0, -10^0, 0^0, 10^0, 20^0, 30^0)$ with FrFT MUSIC spectrum for various array geometries is shown in Figure 3, averaged over G = 100 Monte Carlo simulations. For comparing the RMSE performance with nested and co-prime arrays having 6 elements each given by (33), twos ULA with 12 and 8 elements are also used. It is seen from the plot that the RMSE performance of nested array is comparable with that of ULA with double sensor elements and the two graphs merges with each other beyond SNR = -8 dB. The error is observed more for the co-prime case as compared to the nested structure due to the larger span of hole free difference co-array seen for the nested array [34]. The large virtual linear array thus created by the nested array introduces more spatial samples, in bringing down the RMSE value to zero even at -4 dB SNR.

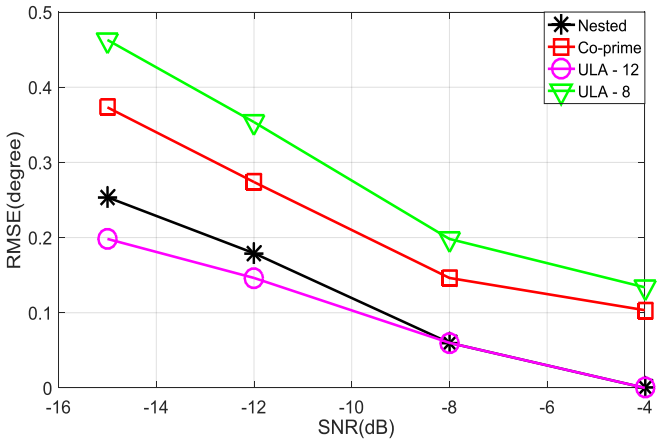

Figure 3. RMSE vs SNR plots of the DoA estimations using two ULAs and two non-ULAs with FrFT MUSIC spectrum.

B. Signal collected using sonar array

The linear chirp signal of 3ms duration shown in Figure 4 (a) is transmitted in the frequency range 2-24 kHz and the transmitter is driven by a 200W linear power amplifier. The back scattered signals are acquired by two rows of eight linear hydrophone array elements with a sampling frequency of 100 kHz. The inter-element separation in each row is 0.0325m. Figure 4 (b) is a plot of the raw data acquired using one of the hydrophones in the array. The whole system called Buried Object Detection Sonar (BODS) for finding targets in

the seabed has been developed by National Institute of Ocean Technology (NIOT), Chennai, India and is mounted in a floating tow body having a speed range of 1-3m/s [36].

The sea trial for testing the BODS system with buried objects was performed at Royapuram Harbor, Chennai, India. A water column depth of 4.5 to 5 m was available at the site. The sediment type at the site was clay mixed with sand and concrete blocks were selected to be buried at the test site about 0.47 m in the seabed. Twenty concrete blocks are arranged in five rows and four columns, where each block has a dimension of 0.3 m x 0.3 m x 0.02 m, hence the entire concrete block set is of the dimension l.5 m x l.2 m x 0.02 m. The raw data from each channel corresponds to 1536 samples. For the current study, the raw data was taken from eight sensor channels with ten block repetitions which altogether makes 1536 x 8 x 10 samples. Also to realize the effect of sparse array, a two level nested array with N = 4 sensors ($N_1 = N_2 = 2$) is considered by taking the data from 1st, 2nd, 3rd and 6th sensors only.

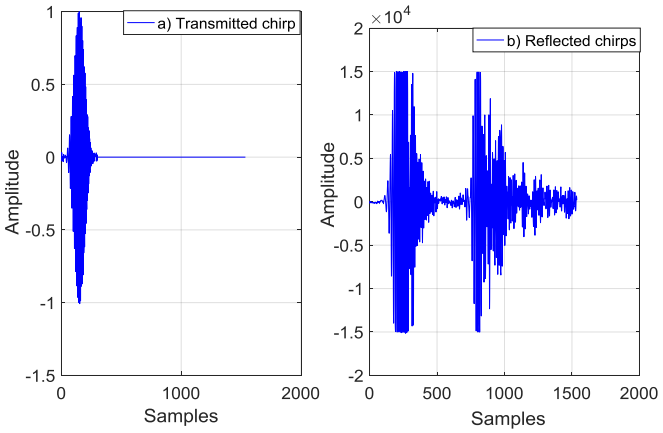

Figure 4. a) Transmitted chirp b) Reflected chirps which is captured using one of the hydrophones in the array.

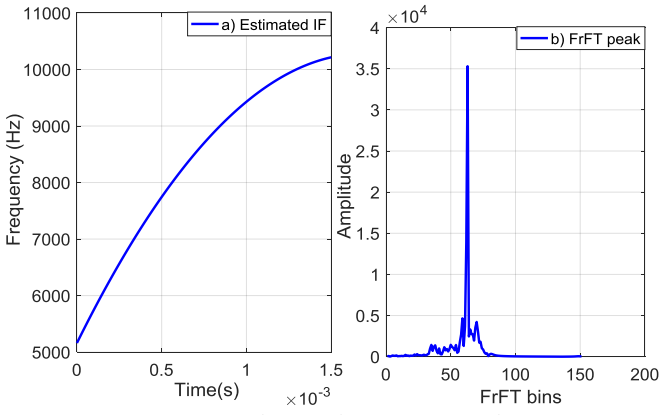

Figure 5. a) Estimated IF for the reflections obtained from the buried concrete blocks b) Peak detection of the reflected chirp obtained from concrete blocks using modified FrFT.

Figure 6 shows the time-frequency plot of the raw data (given by Figure 4 (b)) using PCT approximation with a third order fit. Two strong reflections are marked in the plot, of which the first one is the reflection from the air-water interface and the second one is from the concrete blocks. Figure 5 (a) represents the peak data using PCT after fourth iteration for the concrete reflection alone. It is clear from the plot that the response is non-linear even though the transmitted chirp was linear. This is due to the absorption of some of the frequency contents by the material and the reflected chirp falls in the frequency range of 5 kHz to 10 kHz within a time gap of 1.5 ms. Table 2 also strengthens the above fact which represents the estimated coefficients using third order PCT approximation. The last column shows the polynomial coefficients after fourth iteration and the IF given by $a+2bt+3ct^2$, comes to 10 kHz where t = 1.5 ms. Therefore detection using modified FrFT has to be performed which results in a peak as given by Figure 5 (b).

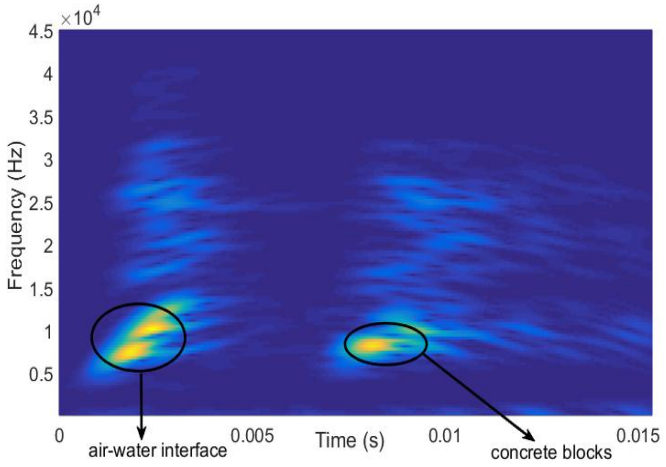

Figure 6. Time-frequency distribution of the raw data given by Figure 4 (b) using polynomial chirplet transform.

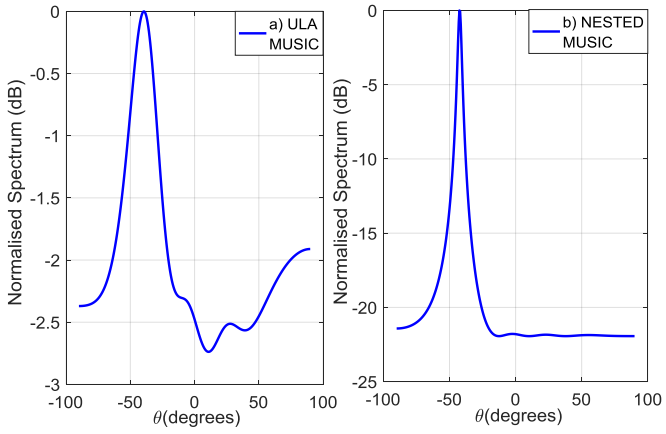

Figure 7. a) DoA estimation of the concrete reflections using MUSIC spectrum with an eight element ULA. b) DoA estimation of the concrete reflections using MUSIC spectrum with a four element nested array.

Table 2. Estimated coefficients using third order polynomial chirplet transform for the concrete reflections.

Coeff.	*1*	*2*	*3*	*4*
a	6223	5549	5160	5008
2b	3265564	5086915	6066146	6483634
3c	-318555610	-1278732825	-1797243811	-2023053641

Finally DoA estimation is performed using the FrFT peak detection and the MUSIC spectra is shown for ULA with 8 sensors (Figure 7 (a)) and nested array (Figure 7 (b)) with 4 sensors. The DoA estimated using an 8 element ULA spreads from -44^0 to -48^0 as given by Figure 7 (a). This is due to the behavior of the object as a surface rather than a point one. Also an improvement in SNR of about 2 dB is observed compared to the traditional FFT method [37] which reflects the power of FrFT detection at deeper penetration. Reduction in beam-width is observed with improved SNR in the case of nested array as shown by Figure 7 (b). This shows the noise resilience property of nested array in comparison with the traditional ULA with more number of sensors. Moreover, the depth of the object can be visualized from Figure 6 using conversion of time information to distance.

VII. CONCLUSION AND FUTURE SCOPE

In this paper, the efficacy and performance of applying FrFT for LFM chirp and modified FrFT for QFM chirp sources using nested and co-prime array is presented, restricting the beam-former to the point where the spectrum peaks. It is seen that more number of chirp sources can be detected with less number of sensors using both nested and co-prime arrays with better accuracy and resolution. The performance has also been tested over a large range of SNR and is observed that nested-MUSIC combination outperforms all other combinations. The effectiveness of the algorithm is experimentally validated using real data obtained from a practical sonar array which highlights the noise resilience property of nested array in comparison with the traditional ULA having more number of sensors. It will be of considerable interest to reduce the effect of mutual coupling as the spacing between the array elements becomes too small. Beam-forming with EFM chirps having Doppler invariant property, which is going beyond FrFT, is another open research area. FrFT beam-forming can also lead to better object classification and underwater imaging as compared to the conventional matched filtering type [36].

ACKNOWLEDGEMENT

The authors would like to thank Dr. M.A. Atmanand, Director- NIOT and Marine Sensor Systems Group for sharing the data set. We would also like to thank the authors of [23] for sharing their Matlab code, which we used to produce the results shown in figures 5 (a) and 6.

REFERENCES

[1] M.A. Richards, "Fundamentals of Radar Signal Processing", McGraw-Hill Publication, India, 2005.
[2] S. Zhou, P. Willett, "Submarine location estimation via a network of detection only sensors", IEEE Trans. Signal Process., Vol. 55, Issue 6, pp. 3104 - 3115, 2007.
[3] H. Krim, M. Viberg, "Two decades of array signal processing research: The parametric approach", IEEE Signal Process. Mag., Vol. 13, pp. 67-94, 1996.
[4] D.H. Johnson, D.E. Dudgeon, "Array Signal Processing Concepts and Techniques", Prentice-Hall, USA, 1993.
[5] J. Capon, "High-resolution frequency-wavenumber spectrum analysis", In the Proceedings of the IEEE, USA, pp. 1408-1418, 1969.
[6] R. Schmidt, "Multiple emitter location and signal parameter estimation", IEEE Trans. on Antennas and Propagation, Vol. 34, Issue 3, pp. 276-280, 1986.
[7] B.D. Rao, K.V.S. Hari, "Performance Analysis of Root-Music", IEEE Trans. on Acoust., Speech and Signal Process., Vol. 37, Issue 12, pp. 1939-1949, 1989.
[8] H.L. Van Trees, "Detection, Estimation, and Modulation Theory-Part IV, Optimum Array Processing", Wiley, USA, 2002.
[9] R.Roy, T.Kailath, "Estimation of signal parameters via rotational invariance techniques," IEEE Trans. Acoust., Speech, Signal Process., Vol. 37, Issue 7, pp. 984-995, 1989.
[10] J.R. Klauder, A.C. Price, S. Darlington, W.J. Albersheim, "The theory and design of chirp radars", Bell Syst. Tech. Jour., Vol. 39, Issue 4, pp. 745-808, 1960.
[11] P.H. Leong, T.D. Abhayapala, T.A. Lamahewa, "Multiple target localization using wideband echo chirp signals", IEEE Trans. Signal Process., Vol.61, Issue 16, pp. 4077-4089, 2013.
[12] I.S. Yetik, A. Nehorai, "Beamforming using the fractional Fourier transform", IEEE Trans. Signal Process., Vol. 51, pp. 1663-1668, 2003.
[13] A.A. Winder, "Sonar system technology", IEEE Trans. Sonics Ultrason., Vol. 22, Issue 5, pp. 291-332, 1975.
[14] M. Wax, T.J. Shan, T. Kailath, "Spatio temporal spectral analysis by eigenstructure methods", IEEE Trans. on Acoust., Speech and Signal Process., Vol. 32, Issue 4, pp. 817-827, 1984.
[15] G. Su, M. Morf, "The signal subspace approach for multiple wideband emitter location", IEEE Trans. on Acoust., Speech and Signal Process., Vol. 31, Issue 6, pp.1502-1522, 1983.
[16] H. Wang, M. Kaveh, "Coherent signal-subspace processing for the detection and estimation of angles of arrival of multiple wide-band sources", IEEE Trans. Acoust., Speech, Signal Process., Vol. 33, Issue 4, pp. 823-831, 1985.
[17] M. A. Doron, A. J. Weiss, "On focusing matrices for wide-band array processing", IEEE Trans. on Signal Process., Vol. 40, Issue 6, pp. 1295-1302, 1992.
[18] E.D. Claudio, R. Parisi, "WAVES: weighted average of signal subspaces for robust wideband direction finding", IEEE Trans. on Signal Process., Vol. 49, Issue 10, pp. 2179-2191, 2001.
[19] Piya Pal, P.P. Vaidyanathan, "A novel autofocusing approach for estimating directions of arrival of wideband signals", In the Proceedings of the 43rd Asilomar Conference on Signals, Systems and Computers, USA, pp. 1663-1667, 2009.
[20] R. Jacob, T. Thomas, A. Unnikrishnan, "Applications of fractional Fourier transform in sonar signal processing", IETE Jour. Res. Vol. 55, pp. 16-27, 2009.

[21] S. Sahay, D. Pande, V. Gadre, P. Sohani, "A novel generalized time-frequency transform inspired by the fractional Fourier transform for higher order chirps", In the Proceedings of the International Conference on Signal Processing (SPCOM), INDIA, pp. 1-5, 2012.
[22] S. Sahay, T. Meghasyam, R.K. Roy, G. Pooniwala, S. Chilamkurthy, V. Gadre, "Parameter estimation of linear and quadratic chirps by employing the fractional Fourier transform and a generalized time frequency transform", Sadhana, Vol. 40, Issue 4, pp. 1049-1075, 2015.
[23] Z. K. Peng, G. Meng, Z. Q. Lang, F. L. Chu, W. M. Zhang, Y. Yang, "Polynomial chirplet transform with application to instantaneous frequency estimation", IEEE Trans. Meas. and Instrum., Vol. 60, Issue 9, pp. 3222-3229, 2011.
[24] S. Mann, S. Haykin, "The chirplet transform: Physical considerations", IEEE Trans. Signal Process., Vol. 43, pp. 2745-2761, 1995.
[25] P. Pal, P. Vaidyanathan, "Nested arrays: A novel approach to array processing with enhanced degrees of freedom", IEEE Trans. Signal Process., Vol. 58, Issue 8, pp. 4167-4181, 2010.
[26] P. Vaidyanathan, P. Pal, "Sparse sensing with co-prime samplers and arrays", IEEE Trans. Signal Process., Vol. 59, Issue 2, pp. 573-586, 2011.
[27] Namias, "The fractional order Fourier transform and its application to quantum mechanics", J. Inst. Math. Appln., Vol. 25, pp. 241-265, 1980.
[28] H.M. Ozaktas, O. Arkan, M.A. Kutay, G. Bozdagi, "Digital computation of the fractional Fourier transform", IEEE Trans. Signal Process., Vol. 44, Issue 9, pp. 2141-2150, 1996.
[29] H. M. Ozaktas, M. A. Kutay, Z. Zalevsky, "The fractional Fourier transform with applications in optics and signal processing", Wiley, USA, 2000.
[30] Y. Cui, K. Liu, J. Wang, "Direction of arrival estimation of coherent wideband LFM signals in multipath environment", In the Proceedings of the International Conf. on Signal Process., USA, pp. 58-61, 2010.
[31] X. Jin, T. Zhang, J. Bai, D. Zhao, "DoA estimation of coherent wideband LFM signals based on fractional Fourier transform and virtual array", In the Proceedings of the IEEE CISP, USA, pp. 4380-4384, 2010.
[32] C. Capus and K. Brown, "Short-time fractional Fourier methods for the time-frequency representation of chirp signals", J. Acoust. Soc. Amer., Vol. 113, Issue 6, pp. 3253-3263, 2003.
[33] C. Capus, Y.Rzhanov, L.Linnett, "Analysis of multiple linear chirp signals", In the Proceedings of the IEE Symposium on Time-Frequency Analysis and Applns., London, pp. 41-47, 2000.
[34] C.L. Liu and P.P. Vaidyanathan, "Remarks on the spatial smoothing step in coarray MUSIC", IEEE Signal Process. Lett., Vol. 22, Issue 9, pp. 1438–1442, 2015.
[35] G. Sreekumar, Leena Mary and A. Unnikrishnan, "Beam-forming of broad-band QFM sigals using generalised time-frequency transform", Elseiver Signal Process., submitted.
[36] S. Bardhan, D. Rajapan, S. Zacharia, M. Eldhose, P.M. Rajeshwari, D.S. Sreedev, C. Kannan , S. Jacob and M.A. Atmanand, "Detection of buried objects using active sonar", IEEE-UT, 2015.
[37] S. Bardhan and S. Jacob, "Experimental observation of DoA estimation algorithms in a tank environment for sonar application", In the Proceedings of the SYMPOL, INDIA, 2015.

Authors Profile

G Sreekumar received the B.Tech in E.C.E from M.G. University, Kerala in 2003 and M.E in Signal Processing from India Institute of Science, Bangalore in 2012. He is currently an Assistant Professor at Rajagiri School of Engineering and Technology, Kochi, Kerala, India in the Department of E.C.E. He is also a part time research scholar at M.G. University. His areas of interest are in digital signal processing and its applications in sensor array signal processing. He is a member of IEEE.

Leena Mary received her Bachelors degree from Mangalore University in 1988. She obtained her M.Tech from Kerala University and Ph.D. from Indian Institute of Technology, Madras, India. Currently she is working as Professor in E.C.E. Dept. at Govt. Engineering College, Idukki, Kerala, India. Her research interests are speech processing, speaker forensics, array processing and neural networks. She has published several research papers which includes a book on Extraction and Representation of Prosody for Speaker, Speech and Language Recognition by Springer. She is a member of IEEE and a life member of ISTE.

A Unnikrishnan graduated from REC (Calicut), India in Electrical Engineering (1975), completed his M.Tech from IIT, Kanpur in Electrical Engineering (1978) and Ph.D from IISc, Bangalore in "Image Data Structures"(1988). He served as Associate Director at Naval Physical and Oceanographic Laboratory, Kochi, which is a premiere Laboratory of D.R.D.O., before joining Rajagiri School of Engineering and Technology as Principal. His field of interests include Sonar Signal Processing, Image Processing and Soft Computing. He has authored about hundred National and International Journal and Conference Papers. He is a Fellow of IETE, IEI and Recognized thesis supervisor of CUSAT and A.P.J. K.T.U., Kerala. He is a member of IEEE, IEEE Computational Engineering Society, Communication Society and Computer Society of India.

